

## AXIONS

Written in August 2007 by C. Hagmann (LLNL), H. Murayama (UC Berkeley), G.G. Raffelt (MPI Physics), L.J. Rosenberg (U. of Washington), and K. van Bibber (LLNL).

**Introduction:** In this section, we list mass and coupling-strength limits for very light neutral scalar or pseudoscalar bosons that couple weakly to normal matter and radiation. Such bosons may arise from a global spontaneously broken U(1) symmetry, resulting in a massless Nambu-Goldstone (NG) boson. If there is a small explicit symmetry breaking, either already in the Lagrangian or due to quantum-mechanical effects such as anomalies, the boson acquires a mass and is called a pseudo-NG boson. Typical examples are axions ( $A^0$ ) [1,2], familons [3] and Majorons [4], associated, respectively, with a spontaneously broken Peccei-Quinn, family and lepton-number symmetry.

A common characteristic among these light bosons  $\phi$  is that their coupling to Standard-Model particles is suppressed by the energy scale that characterizes the symmetry breaking, *i.e.*, the decay constant  $f$ . The interaction Lagrangian is

$$\mathcal{L} = f^{-1} J^\mu \partial_\mu \phi, \quad (1)$$

where  $J^\mu$  is the Noether current of the spontaneously broken global symmetry. If  $f$  is very large, these new particles interact very weakly. Conversely, detecting them would provide a window to physics far beyond what can be probed at accelerators.

The interest in global symmetries and the associated NG bosons has somewhat waned except for the case of axions where it has held steady since they were proposed 30 years ago. This is because the Peccei-Quinn (PQ) mechanism remains perhaps the most credible scheme to preserve  $CP$  in QCD; axions are a plausible candidate for the cold dark matter of the universe and they are searched for in experiments with a realistic chance of discovery. Originally it was assumed that the PQ scale  $f_A$  was related to the electroweak symmetry-breaking scale  $v_{\text{weak}} = (\sqrt{2}G_F)^{-1/2} = 247$  GeV. However, the associated “standard” and “variant” axions were quickly excluded, leaving

“invisible axions” with  $f_A \gg v_{\text{weak}}$  as the main possibility. We refer to the Listings for limits on standard and variant axions, whereas here we focus primarily on very low-mass, very weakly-interacting axions and axion-like particles.

## I. THEORY

***I.1 Peccei-Quinn mechanism and axions:*** QCD includes a  $CP$ -violating Lagrangian  $\mathcal{L}_\Theta = \bar{\Theta} (\alpha_s/8\pi) G^{\mu\nu a} \tilde{G}_{\mu\nu}^a$ , where  $-\pi \leq \bar{\Theta} \leq +\pi$  is the effective  $\Theta$  parameter after diagonalization of the quark masses,  $G$  is the color field strength tensor, and  $\tilde{G}$  its dual. Experimental limits on the neutron electric dipole moment [5] imply  $|\bar{\Theta}| \lesssim 10^{-10}$  even though  $\bar{\Theta} = \mathcal{O}(1)$  is otherwise completely satisfactory. The spontaneously broken global Peccei-Quinn symmetry  $U(1)_{\text{PQ}}$  was introduced to solve this “strong  $CP$  problem” [1], and an axion is the pseudo-NG boson of  $U(1)_{\text{PQ}}$  [2]. This symmetry is exact on the classical level, but is broken quantum mechanically due to the axion’s anomalous triangle coupling to gluons,

$$\mathcal{L} = \left( \bar{\Theta} - \frac{\phi_A}{f_A} \right) \frac{\alpha_s}{8\pi} G^{\mu\nu a} \tilde{G}_{\mu\nu}^a, \quad (2)$$

where  $\phi_A$  is the axion field and  $f_A$  the axion decay constant. Color anomaly factors have been absorbed in the normalization of  $f_A$  which is defined by this Lagrangian. Thus normalized,  $f_A$  is the quantity that enters all low-energy phenomena [6]. Non-perturbative effects induce a potential for  $\phi_A$  whose minimum is at  $\phi_A = \bar{\Theta} f_A$ , thereby canceling the  $\bar{\Theta}$  term in the QCD Lagrangian, and thus restoring the  $CP$  symmetry.

The resulting axion mass is given by  $m_A f_A \approx m_\pi f_\pi$  where  $m_\pi = 135$  MeV and  $f_\pi \approx 92$  MeV is the pion decay constant. In more detail one finds

$$m_A = \frac{z^{1/2}}{1+z} \frac{f_\pi m_\pi}{f_A} = \frac{0.60 \text{ meV}}{f_A/10^{10} \text{ GeV}}, \quad (3)$$

where  $z = m_u/m_d$  is the up/down quark-mass ratio. For this numerical estimate we used a canonical value of  $z = 0.56$  [7], but it could vary in the range  $z = 0.3\text{--}0.6$  [8].

In the original axion model,  $f_A \sim v_{\text{weak}}$  [1,2]. Tree-level flavor conservation fixes the axion mass and its couplings in

terms of a single parameter  $\tan\beta$ , the ratio of the vacuum expectation values of the two Higgs fields that appear as a minimal ingredient. This “standard axion” is excluded after extensive experimental searches [9]. A reported observation of a narrow-peak structure in positron spectra from heavy ion collisions [10] suggested an axion-like particle of mass 1.8 MeV that decays into  $e^+e^-$ , but extensive searches for the  $A^0(1.8\text{ MeV})$  ended negative. “Variant axion models” were proposed which keep  $f_A \sim v_{\text{weak}}$  while dropping the constraint of tree-level flavor conservation [11], but these models are also excluded [12].

Axions with  $f_A \gg v_{\text{weak}}$  evade all existing experimental limits. Two classes of models are often discussed in the literature. In “hadronic axion models,” one introduces new heavy quarks carrying the  $U(1)_{\text{PQ}}$  charge, leaving the usual quarks and leptons without any tree-level axion couplings. The prototype is the KSVZ model [13], which has the additional property that the heavy quarks are electrically neutral. Another model class simply requires a minimum of two Higgs doublets with the usual quarks and leptons carrying PQ charges, the prototype being the DFSZ model [14]. All of these models contain at least one electroweak singlet scalar boson, which acquires a vacuum expectation value and thereby breaks the PQ symmetry. The KSVZ and DFSZ models are frequently used as generic examples, but other models exist where both heavy quarks and Higgs doublets carry PQ charges. In one recent example, the PQ charges of all fields were derived within a superstring model [15].

***1.2 Model-dependent axion couplings:*** Although the generic axion interactions scale approximately with  $f_\pi/f_A$  from the corresponding  $\pi^0$  couplings, there are non-negligible model-dependent factors and uncertainties. The axion’s two-photon interaction plays a key role for many searches,

$$\mathcal{L}_{A\gamma\gamma} = \frac{G_{A\gamma\gamma}}{4} F_{\mu\nu} \tilde{F}^{\mu\nu} \phi_A = -G_{A\gamma\gamma} \mathbf{E} \cdot \mathbf{B} \phi_A. \quad (4)$$

Here,  $F$  is the electromagnetic field-strength tensor,  $\tilde{F}$  its dual, and  $\mathbf{E}$  and  $\mathbf{B}$  the electric and magnetic fields, respectively. The

coupling constant is

$$\begin{aligned} G_{A\gamma\gamma} &= \frac{\alpha}{2\pi f_A} \left( \frac{E}{N} - \frac{2}{3} \frac{4+z}{1+z} \right) \\ &= \frac{\alpha}{2\pi} \left( \frac{E}{N} - \frac{2}{3} \frac{4+z}{1+z} \right) \frac{1+z}{z^{1/2}} \frac{m_A}{m_\pi f_\pi}, \end{aligned} \quad (5)$$

where  $E$  and  $N$ , respectively, are the electromagnetic and color anomalies of the axial current associated with the axion. In grand unified models, and notably in the DFSZ case [14], we have  $E/N = 8/3$ , whereas  $E/N = 0$  for KSVZ [13] if the electric charge of the new heavy quark is taken to vanish. However, in general,  $E/N$  is not known so that for fixed  $f_A$ , a broad range of  $G_{A\gamma\gamma}$  values is possible [16].

Axions or axion-like particles with a two-photon vertex decay with a rate

$$\begin{aligned} \Gamma_{A \rightarrow \gamma\gamma} &= \frac{G_{A\gamma\gamma}^2 m_A^3}{64 \pi} \\ &= \frac{\alpha^2}{256 \pi^3} \left( \frac{E}{N} - \frac{2}{3} \frac{4+z}{1+z} \right)^2 \frac{(1+z)^2}{z} \frac{m_A^5}{m_\pi^2 f_\pi^2} \\ &= 1.1 \times 10^{-24} \text{ s}^{-1} \left( \frac{m_A}{\text{eV}} \right)^5, \end{aligned} \quad (6)$$

where the first expression is for general pseudoscalars, the second for axions, and the third assumes  $z = 0.56$  and  $E/N = 0$ . Axions decay faster than the age of the universe if  $m_A \gtrsim 20$  eV.

The interaction with fermions  $f$  has a derivative structure so that it is invariant under a constant shift  $\phi_A \rightarrow \phi_A + \phi_0$  as behooves a NG boson,

$$\mathcal{L}_{Aff} = \frac{C_f}{2f_A} \bar{\Psi}_f \gamma^\mu \gamma_5 \Psi_f \partial_\mu \phi_A \quad \text{or} \quad -i \frac{C_f m_f}{f_A} \bar{\Psi}_f \gamma_5 \Psi_f \phi_A. \quad (7)$$

Here,  $\Psi_f$  is the fermion field,  $m_f$  its mass, and  $C_f$  a model-dependent numerical coefficient. The dimensionless combination  $g_{Aff} \equiv C_f m_f / f_A$  plays the role of a Yukawa coupling and  $\alpha_{Aff} \equiv g_{Aff}^2 / 4\pi$  of a ‘‘fine-structure constant.’’ The pseudoscalar form is usually equivalent to the derivative structure, but one has to be careful in processes where two NG bosons are attached to one fermion line, for example in the context of axion emission by nucleon bremsstrahlung [17].

Hadronic axions do not couple to ordinary quarks and leptons at tree level. In the DFSZ model [14], the coupling coefficient to electrons is

$$C_e = \frac{\cos^2 \beta}{3}, \quad (8)$$

where  $\tan \beta$  is the ratio of two Higgs vacuum expectation values that are generic to this and similar models.

The nucleon couplings  $C_{n,p}$  are related to nucleon axial-vector current matrix elements by generalized Goldberger-Treiman relations,

$$\begin{aligned} C_p &= (C_u - \eta)\Delta u + (C_d - \eta z)\Delta d + (C_s - \eta w)\Delta s, \\ C_n &= (C_u - \eta)\Delta d + (C_d - \eta z)\Delta u + (C_s - \eta w)\Delta s. \end{aligned} \quad (9)$$

Here,  $\eta = (1 + z + w)^{-1}$  with  $z = m_u/m_d$  and  $w = m_u/m_s \ll z$ .  $\Delta q$  represents the axial-vector current couplings to the proton by  $\Delta q S_\mu = \langle p | \bar{q} \gamma_\mu \gamma_5 q | p \rangle$ , where  $S_\mu$  is the proton spin.

Neutron beta decay and strong isospin symmetry considerations imply  $\Delta u - \Delta d = F + D = 1.267 \pm 0.0035$ , whereas hyperon decays and flavor SU(3) symmetry imply  $\Delta u + \Delta d - 2\Delta s = 3F - D = 0.585 \pm 0.025$ . The strange-quark contribution is  $\Delta s = -0.08 \pm 0.01_{\text{stat}} \pm 0.05_{\text{syst}}$  from the COMPASS experiment [18], and  $\Delta s = -0.085 \pm 0.008_{\text{exp}} \pm 0.013_{\text{theor}} \pm 0.009_{\text{evol}}$  from HERMES [19], in agreement with each other and with an early estimate of  $\Delta s = -0.11 \pm 0.03$  [20]. We thus adopt

$$\begin{aligned} \Delta u &= +0.841 \pm 0.020, \\ \Delta d &= -0.426 \pm 0.020, \\ \Delta s &= -0.085 \pm 0.015, \end{aligned} \quad (10)$$

which are very similar to what was used in the axion literature.

The uncertainty of the axion-nucleon couplings is dominated by the uncertainty  $z = 0.3\text{--}0.6$  that we mentioned earlier. For hadronic axions  $C_{u,d,s} = 0$ , so that  $C_p = -0.55$  and  $C_n = +0.14$ , if  $z = 0.3$  and  $C_p = -0.37$  and  $C_n = -0.05$  if  $z = 0.6$ . While it is well possible that  $C_n = 0$ ,  $C_p$  does not vanish within the plausible  $z$  range. In the DFSZ model,  $C_u = \frac{1}{3} \sin^2 \beta$  and  $C_d = \frac{1}{3} \cos^2 \beta$ . Even with the large  $z$ -uncertainty,  $C_n$  and  $C_p$  never vanish simultaneously. An extreme case is  $\cos^2 \beta = 0$ , where  $C_p = 0$  for  $z = 0.3$ , but in this case  $C_n = -0.27$ .

The axion–pion interaction is given by the Lagrangian [21]

$$\mathcal{L}_{A\pi} = \frac{C_{A\pi}}{f_\pi f_A} (\pi^0 \pi^+ \partial_\mu \pi^- + \pi^0 \pi^- \partial_\mu \pi^+ - 2\pi^+ \pi^- \partial_\mu \pi^0) \partial_\mu \phi_A. \quad (11)$$

In hadronic axion models, the coupling constant is

$$C_{A\pi} = \frac{1 - z}{3(1 + z)}. \quad (12)$$

In general the chiral symmetry-breaking Lagrangian contributes an additional piece to  $\mathcal{L}_{A\pi}$  proportional to  $(m_\pi^2/f_\pi f_A) (\pi^0 \pi^0 + 2\pi^- \pi^+) \pi^0 \phi_A$ . For hadronic axions, this term vanishes identically, in contrast, for example, to the DFSZ model (Roberto Peccei, private communication).

## II. LABORATORY SEARCHES

**II.1 Photon regeneration:** Searching for “invisible axions” in laboratory experiments is extremely challenging. The most promising approaches use the axion-two-photon vertex, allowing axions and photons to convert into each other in the presence of external electric or magnetic fields [22]. When the external field is the Coulomb field of a charged particle, the conversion is best viewed as an ordinary scattering process,  $\gamma + Ze \leftrightarrow Ze + A$ , called Primakoff effect in analogy to the corresponding  $\pi^0$  process [23]. In the other extreme of a macroscopic field, usually a large-scale  $B$ -field, the momentum transfer is small, the interaction coherent over a large distance, and the conversion is best viewed as an axion–photon oscillation phenomenon in analogy to neutrino-flavor oscillations [24]. The search for solar axions with the “helioscope technique” [22], or for dark-matter axions with the “haloscope technique” [22], are based on this concept and will be discussed in the sections on stellar and cosmological axions below, whereas here we concentrate on pure laboratory experiments that do not require astrophysical sources.

Photons propagating through a transverse magnetic field, with incident  $\mathbf{E}$  and magnet  $\mathbf{B}$  parallel, may convert into axions. For light axions with  $m_A^2 L/2\omega \ll 2\pi$ , where  $L$  is the length of the magnetic field conversion region and  $\omega$  the photon energy, the resultant axion beam is collinear and coherent with the incident photon beam, and the conversion probability  $\Pi$  is

given by  $\Pi \sim (1/4)(G_{A\gamma\gamma}BL)^2$ . A practical realization of this concept is a laser beam propagating down the bore of a long superconducting dipole magnet (like the bending magnets in high-energy accelerators). If another such dipole magnet is in line with the first, with an optical barrier separating the two, then photons may be regenerated and detected in the second magnet from the pure axion beam [25]. The overall probability  $P(\gamma \rightarrow A \rightarrow \gamma) = \Pi^2$ .

Such an experiment has been carried out, utilizing two magnets of length  $L = 4.4$  m and  $B = 3.7$  T. For  $m_A < 1$  meV, the coupling was found to be constrained by  $G_{A\gamma\gamma} < 6.7 \times 10^{-7}$  GeV $^{-1}$  at 95% CL [26]. More recently, the Light Pseudo Scalar Search project (LIPSS) collaboration has taken data at the Jefferson Laboratory free-electron infrared laser facility. The claimed sensitivity of their detector is  $G_{A\gamma\gamma} = 1.7 \times 10^{-6}$  GeV $^{-1}$  [27]. Another recent experiment uses a pulsed laser with similar sensitivity [28]. Most recently, the GammeV Particle Search Experiment experiment at FNAL has reported a  $3\sigma$  constraint of  $G_{A\gamma\gamma} < 3.2 \times 10^{-7}$  GeV $^{-1}$  in the limit  $m_A = 0$  [29]. Other experiments that are planned or under construction include the Axion-Like Particle Search experiment (ALPS) at DESY, and the Optical Search for QED vacuum magnetic birefringence experiment at CERN.

A new concept has been proposed, resonantly-enhanced photon regeneration, which may enable searches into unexplored regions of axion-photon couplings [30]. In this scheme, both the production and detection magnets are within Fabry-Perot optical cavities and actively locked in frequency. The enhancement is  $P^{\text{res}}(\gamma \rightarrow a \rightarrow \gamma) = (2\mathcal{F}\mathcal{F}'/\pi^2) \times P^{\text{non-res}}$ , where  $\mathcal{F}$  and  $\mathcal{F}'$  are the finesse of the two optical cavities. Feasibly, the resonant enhancement could be of order  $10^{(10-12)}$ , leading to improvements in sensitivity in  $G_{A\gamma\gamma}$  of  $10^{(2.5-3)}$ .

**II.2 Photon polarization:** An alternative to regenerating the lost photons is to use the beam itself to detect the  $B$ -field-induced photon-axion conversion: the polarization of light propagating through a transverse magnetic field suffers dichroism and birefringence [31]. Dichroism: The  $E_{\parallel}$  component, but not the  $E_{\perp}$  component, will be depleted by the production of

axions, and thus there will be in general a small rotation of the polarization vector of linearly-polarized light. The effect will be constant for all sufficiently light axions, such that the oscillation length is much longer than the magnet  $m_A^2 L/2\omega \ll 2\pi$ . For heavier axions, the effect oscillates and diminishes as  $m_A$  increases, and vanishes for  $m_A > \omega$ . Birefringence: This rotation occurs because there is mixing of virtual axions in the  $E_{\parallel}$  state, but not for the  $E_{\perp}$  state. Hence, initially linearly polarized light will become elliptically polarized. Higher-order QED also induces vacuum birefringence. A search for these effects was performed on the same dipole magnets in the early experiment above [32]. Any effect increases linearly when the beam passes through an optical cavity within the magnet. The dichroic rotation gave a stronger limit than the ellipticity rotation:  $G_{A\gamma\gamma} < 3.6 \times 10^{-7} \text{ GeV}^{-1}$  at 95% CL for  $m_A < 5 \times 10^{-4} \text{ eV}$ . The ellipticity rotation limits are better at higher masses, as they fall off smoothly and do not terminate at  $m_A$ .

In 2006, a publication by the PVLAS collaboration reported a signature of magnetically induced vacuum dichroism, which could have been interpreted as evidence for a light pseudoscalar with a mass of 1–1.5 meV and a photon coupling of  $(1.6\text{--}5) \times 10^{-6} \text{ GeV}^{-1}$  [33]. This result was problematic from several points of view, not the least of which was the difficulty in reconciling the magnitude of the signal with the much more restrictive limits on  $G_{A\gamma\gamma}$  from the Sun, horizontal branch stars, and CAST (see below). Furthermore, the PVLAS data themselves evidenced large systematic errors of unknown origin. More recently, the PVLAS collaboration issued a report retracting their earlier findings. They conclude the effects were instrumental artifacts, with no evidence for new physics [34].

**II.3 Long-range forces:** New bosons would mediate long-range forces, which are severely constrained by “fifth force” experiments [35]. These experiments, notably those looking for new mass-spin couplings, provide significant constraints on axion-like particles [36,37]. The limits on the product of couplings at the mass- and spin-coupled interaction vertices (Figure 1) may be related to limits on the DFSZ model [36].

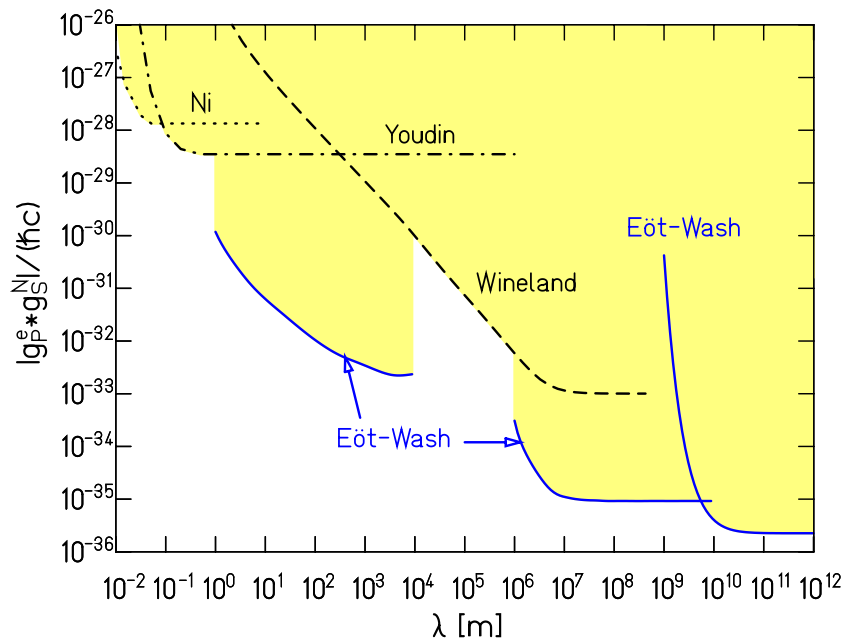


**Figure 1:** Short-distance gravity upper limits [37] on the product of mass- and spin-vertex couplings as a function of the interaction range  $\lambda$ ; the shaded region is excluded at 95% confidence. Figure courtesy E. Adelberger.

In summary, pure laboratory searches for invisible axions have not yet provided useful limits on plausible models. Photon propagation or long-range force experiments are only sensitive for small  $m_A$ , so that the corresponding coupling strengths that scale with  $f_A^{-1} \approx m_A/m_\pi f_\pi$  are too small to be detected. However, these efforts provide constraints on general low-mass bosons, and have searched for axions of non-standard masses and couplings.

### III. AXIONS FROM ASTROPHYSICAL SOURCES

**III.1 Stellar energy-loss limits:** Low-mass weakly-interacting particles (neutrinos, gravitons, axions, baryonic or leptonic gauge bosons, *etc.*) are produced in hot astrophysical plasmas, and can thus transport energy out of stars. The coupling strength of the particles with normal matter and radiation

is bounded by the constraint that stellar-evolution lifetimes or energy-loss rates not conflict with observation [38–40].

We begin with our Sun and concentrate on hadronic axion models. The dominant production is by the Primakoff process  $\gamma + Ze \rightarrow Ze + A$ , where photons convert into axions in the electric fields of the charged particles in the plasma. Integrating over a standard solar model, one finds an axion luminosity [53]

$$L_A = G_{10}^2 1.85 \times 10^{-3} L_\odot, \quad (13)$$

where  $G_{10} = G_{A\gamma\gamma} \times 10^{10}$  GeV. The maximum of the spectrum is at 3.0 keV, the average at 4.2 keV, and the number flux at Earth is  $G_{10}^2 3.75 \times 10^{11} \text{ cm}^{-2} \text{ s}^{-1}$ .

The axion losses lead to an enhanced consumption of nuclear fuel. The standard Sun is halfway through its hydrogen-burning phase so that the solar axion luminosity cannot significantly exceed its photon luminosity  $L_\odot$ . For a more refined constraint, we note that a model of the present-day Sun, with the integrated effect of axion losses taken into account, differs from a standard solar model for sufficiently large values of the coupling constant. The modified sound-speed profile can be diagnosed by helioseismology, providing a conservative limit  $G_{10} \lesssim 10$ , corresponding to  $L_A \lesssim 0.20 L_\odot$  [41]. More recent determinations of the solar metal abundances have spoiled the almost perfect agreement between standard solar models and helioseismology [42], a problem that is not yet resolved. However, the axion limit probably remains unaffected.

The energy loss by solar axion emission requires enhanced nuclear burning, and thus an increased temperature. Self-consistent solar models with axion losses reveal that  $G_{10} = 4.5$  causes a 20% increase of the solar  $^8\text{B}$  neutrino flux [41]. The measured all-flavor  $^8\text{B}$  solar neutrino flux is  $4.94 \times 10^6 \text{ cm}^{-2} \text{ s}^{-1}$  with an uncertainty of about 8.8% [43]. The old standard solar model predictions were 5.7–5.9 in the same units, whereas the new metal abundances imply 4.5–4.6, each time with a 16% “theoretical  $1\sigma$  error” [42]. Therefore, the measured neutrino fluxes imply a limit  $G_{10} \lesssim 5$ , corresponding to  $L_A \lesssim 0.04 L_\odot$ .

A more restrictive limit on  $G_{A\gamma\gamma}$  arises from globular-cluster (GC) stars. A GC is a gravitationally bound system of a homogeneous population of low-mass stars, allowing for detailed tests of stellar-evolution theory. The stars on the horizontal branch (HB) in the color-magnitude diagram have reached helium burning, where their core (mass  $\sim 0.5 M_\odot$ , density  $\sim 10^4 \text{ g cm}^{-3}$ , temperature  $\sim 10^8 \text{ K}$ ) generates energy by fusing helium to carbon and oxygen with a core-averaged energy release of about  $80 \text{ erg g}^{-1} \text{ s}^{-1}$ . The core-averaged Primakoff axion loss rate is about  $G_{10}^2 30 \text{ erg g}^{-1} \text{ s}^{-1}$ . The main effect is accelerated consumption of helium, and thus a reduction of the HB lifetime by about  $80/(80 + 30 G_{10}^2)$ . The HB lifetime is measured relative to the red-giant branch (RGB) evolutionary time scale by comparing the number of HB stars with the number of RGB stars. This number ratio agrees with expectations within 20–40% in any one of 15 studied GCs [44]. Compounding the results of all 15 GCs, the agreement is within about 10% [39]. A reasonably conservative limit is

$$G_{A\gamma\gamma} \lesssim 1 \times 10^{-10} \text{ GeV}^{-1}, \quad (14)$$

although an objective error budget is not available.

We translate this nominal constraint on the axion-photon interaction strength to  $f_A > 2.3 \times 10^7 \text{ GeV}$  (and thus  $m_A < 0.3 \text{ eV}$ ), using  $z = 0.56$  and  $E/N = 0$  as in the KSVZ model, and show the excluded range in Figure 2. For the DFSZ model with  $E/N = 8/3$ , the corresponding limits are slightly less restrictive,  $f_A > 0.8 \times 10^7 \text{ GeV}$  (and thus  $m_A < 0.7 \text{ eV}$ ). The exact high-mass end of the exclusion range has not been determined. We note that the relevant temperature is around 10 keV, and the average photon energy is therefore around 30 keV. The excluded  $m_A$  range thus certainly extends beyond the shown 100 keV.

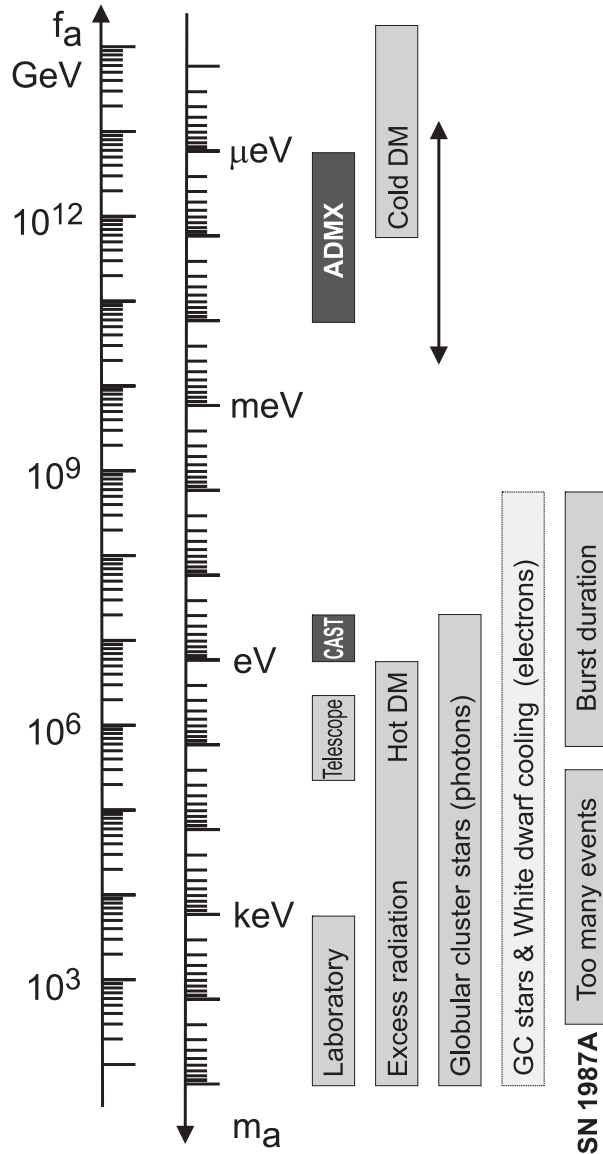


**Figure 2:** Exclusion and experimental search ranges as described in the text. Limits on coupling strengths are translated into limits on  $m_A$  and  $f_A$  using  $z = 0.56$  and the KSVZ values for the coupling strengths. The “Laboratory” bar is a rough representation of the exclusion range for standard or variant axions. The “GC stars and white-dwarf cooling” range uses the DFSZ model with an axion-electron coupling corresponding to  $\cos^2 \beta = 1/2$ . The Cold Dark Matter exclusion range is particularly uncertain. We show the benchmark case from the misalignment mechanism.

In models where axions couple directly to electrons, processes of the form  $\gamma + e^- \rightarrow e^- + a$  and  $e^- + Ze \rightarrow Ze + e^- + a$  are more efficient than the Primakoff process. Moreover, bremsstrahlung is efficient in degenerate stars such as white dwarfs, where the Primakoff and Compton processes are suppressed by the large photon plasma frequency. One limit comes from GC stars where the enhanced energy losses would delay helium ignition so that the tip of the RGB would be brighter than observed [45], implying  $\alpha_{Aee} \lesssim 0.5 \times 10^{-26}$ . Axion emission would also enhance white-dwarf cooling, leading to a similar limit  $\alpha_{Aee} \lesssim 1 \times 10^{-26}$  from the white-dwarf luminosity function [46]. For pulsationally unstable white dwarfs (ZZ Ceti stars), the period decrease  $\dot{P}/P$  is a measure of the cooling speed. A well-studied case is the star G117–B15A, where  $\dot{P}/P$  has been measured, implying [47]

$$\alpha_{Aee} < 1.3 \times 10^{-27} \quad (15)$$

at a statistical 95% CL. (We have corrected the published limit for an apparent misprint.) This result is equivalent to  $g_{Aee} < 1.3 \times 10^{-13}$  or in the DFSZ model to  $f_A > 1.3 \times 10^9 \text{ GeV} \cos^2 \beta$  and  $m_A < 4.5 \text{ meV} / \cos^2 \beta$ . We show these constraints in Figure 2 for  $\cos^2 \beta = 1/2$ .

Similar constraints are provided by the neutrino signal of the supernova SN 1987A. Several detectors registered together about two dozen events spread over about 10 s, showing that the burst duration was not significantly shortened by a new energy-loss channel. Numerical simulations for a variety of cases, including axions and Kaluza-Klein gravitons, reveal that the energy-loss rate of a nuclear medium at the density  $3 \times 10^{14} \text{ g cm}^{-3}$  and temperature 30 MeV should not exceed about  $1 \times 10^{19} \text{ erg g}^{-1} \text{ s}^{-1}$  [39]. Translating this nominal criterion into a limit on the axion-nucleon coupling depends on a calculation of bremsstrahlung emission  $N + N \rightarrow N + N + a$  in a nuclear medium. The energy loss rate per unit mass is found to be  $(C_N/2f_A)^2 (T^4/\pi^2 m_N) F$ . Here  $F$  is a numerical factor that represents an integral over the dynamical spin-density structure function, because axions couple to the nucleon spin and thus are essentially emitted by the fluctuating nuclear spins of the dense

medium. In a dilute medium,  $F$  would have the interpretation of  $\Gamma/2T$  with  $\Gamma$  a typical nucleon spin fluctuation rate. For realistic conditions, even after considerable effort, one is limited to a heuristic estimate leading to  $F \approx 1$  [40].

The SN 1987A limits are of particular interest for hadronic axions where the bounds on  $\alpha_{Aee}$  are moot. Therefore, we use  $C_p = -0.4$  and  $C_n = 0$ . We use an initial proton fraction of 0.3 to scale the emission rate to the proton density. With  $F = 1$  and  $T = 30$  MeV we find [40]

$$f_A \gtrsim 4 \times 10^8 \text{ GeV} \quad \text{and} \quad m_A \lesssim 16 \text{ meV}. \quad (16)$$

If axions interact sufficiently strongly they are trapped, like neutrinos, so that only about three orders of magnitude in  $g_{ANN}$  or  $m_A$  are excluded by the burst duration. We show the excluded range somewhat schematically in Figure 2. For even larger couplings, the axion flux would have been negligible, yet it would have triggered additional events in the detectors, excluding a further range of couplings [48]. A possible gap between the exclusion ranges of these two SN 1987A arguments was discussed as the “hadronic axion window” under the assumption that  $G_{A\gamma\gamma}$  was anomalously small [49]. This range is now excluded by the cosmic structure-formation arguments to be discussed in the section on cosmological axions.

**III.2 Searches for solar axions:** Instead of using stellar energy losses to derive limits on axion parameters, one can also search directly for these fluxes in the laboratory, notably those from our Sun. The main experimental focus has been on axion-like particles with a two-photon vertex. They are produced by the Primakoff process with a flux given by Equation 13, and can be detected at Earth with the reverse process in a macroscopic  $B$ -field (“axion helioscope”) [22]. Viewing this re-conversion as a particle oscillation process, we note that the average energy of solar axions is 4.2 keV, implying a photon-axion oscillation length in vacuum of  $2\pi(2\omega/m_A^2) \sim \mathcal{O}(1 \text{ mm})$ , precluding the vacuum mixing from achieving its theoretical maximum in any practical magnet. However, one can endow the photon with an effective mass in a gas,  $m_\gamma = \omega_{\text{plas}}$ , thus matching the axion and photon dispersion relations [50].

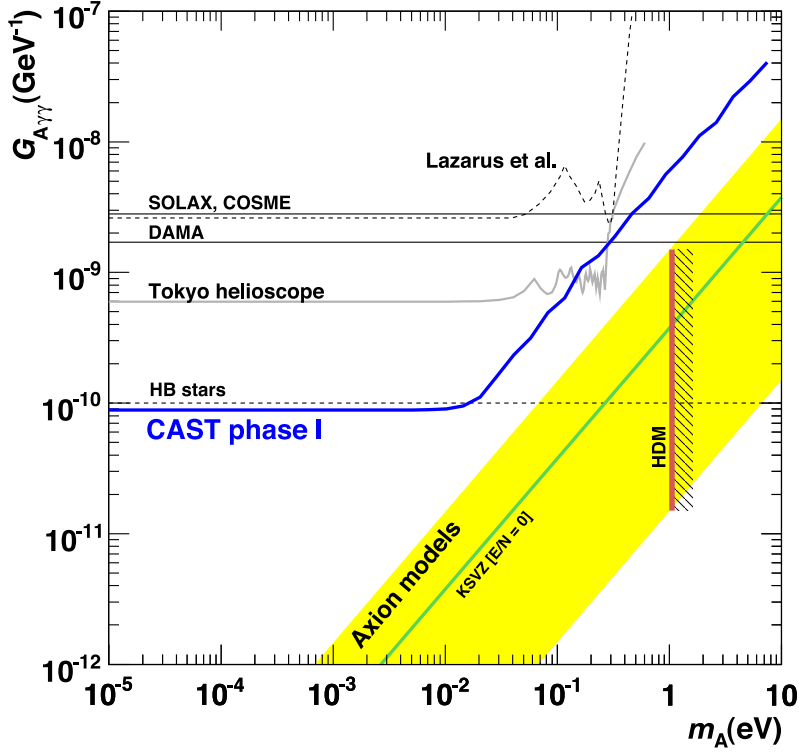


**Figure 3:** Solar-axion exclusion plot in the  $G_{A\gamma\gamma}$ - $m_A$ -plane for axion-like particles [53]. For small masses, the most restrictive limit is from CAST-I [53], and is shown with previous helioscopes Lazarus *et al.* [51] and the Tokyo helioscope [52]. Also shown are constraints from experiments using the Bragg technique SOLAX [55], COSME [56], and DAMA [57]. The vertical red line (HDM) is the hot dark-matter limit [64]. The yellow band represents models with  $|E/N - 1.92|$  in the range 0.07–7, while the green solid line corresponds to the KSVZ case.

An early implementation of these ideas was carried out using a conventional dipole magnet, with a conversion volume of variable-pressure gas with a xenon proportional chamber as x-ray detector [51]. The conversion magnet was fixed in orientation and collected data for about 1000 s/day. Axions were excluded for  $G_{A\gamma\gamma} < 3.6 \times 10^{-9} \text{ GeV}^{-1}$  for  $m_A < 0.03 \text{ eV}$ , and  $G_{A\gamma\gamma} <$

$7.7 \times 10^{-9} \text{ GeV}^{-1}$  for  $0.03 < m_A < 0.11 \text{ eV}$  at 95% CL. Later, the Tokyo axion helioscope used a superconducting magnet on a tracking mount, viewing the Sun continuously. They reported  $G_{A\gamma\gamma} < 6 \times 10^{-10} \text{ GeV}^{-1}$  for  $m_A < 0.3 \text{ eV}$  [52]. The exclusion ranges are shown in Figure 3.

The most recent helioscope CAST (CERN Axion Solar Telescope) uses a decommissioned LHC dipole magnet on a tracking mount and is actively taking data. The hardware includes grazing-incidence x-ray optics with solid-state x-ray detectors, as well as a novel x-ray Micromegas position-sensitive gaseous detector. CAST has established a 95% CL limit  $G_{A\gamma\gamma} < 8.8 \times 10^{-11} \text{ GeV}^{-1}$  for  $m_a < 0.02 \text{ eV}$  [53]. To cover larger masses and to “cross the axion line,” the conversion region in the magnet bores is filled with a gas at varying pressure. The runs with  $^4\text{He}$  gas are complete and cover masses up to about 0.4 eV, but exact limits on  $G_{A\gamma\gamma}$  in this range have not yet been established [54]. Forthcoming runs with  $^3\text{He}$  gas will explore axion masses up to 1.16 eV within about 3 years.

Other Primakoff searches for solar axions have been carried out using crystal detectors, exploiting the coherent conversion of axions into photons when the axion angle of incidence satisfies a Bragg condition with a crystalline plane. Limits from SOLAX [55], COSME [56], and DAMA [57] are summarized in Figure 4.

Another idea is to look at the Sun with an x-ray satellite when the Earth is in between. Solar axions would be converted in the Earth magnetic field on the far side relative to the Sun into x-rays, and could be picked up by the detector [58]. The sensitivity to  $G_{A\gamma\gamma}$  could be comparable to CAST, but only for much smaller  $m_A$ .

**III.3 Conversion of astrophysical photon fluxes:** Large-scale magnetic fields exist in astrophysics that can induce axion–photon oscillations. In practical cases,  $B$  is much smaller than the laboratory fields used, for example, in helioscopes, whereas the conversion region  $L$  is much larger. Therefore, while the product  $BL$  can be large, any realistic sensitivity is usually restricted to very low-mass particles, far away from the “axion line” in a plot like Figure 3.

One example is SN 1987A, which would have emitted a burst of axion-like particles due to the Primakoff production in its core. They would have partially converted into  $\gamma$ -rays in the galactic  $B$ -field. The absence of a  $\gamma$ -ray burst in coincidence with the SN 1987A neutrino burst provides a limit  $G_{A\gamma\gamma} \lesssim 1 \times 10^{-11} \text{ GeV}^{-1}$  for  $m_A \lesssim 10^{-9} \text{ eV}$  [59]. This is the most restrictive limit for very small  $m_A$ .

Axion-like particles from other stars could be converted to photons in astrophysical  $B$ -fields, but no tangible new limits or signatures seem to have appeared.

Conversely, photons from distant sources could be converted to axion-like particles, depleting the original flux, thereby dimming the sources. This mechanism was proposed as an alternative explanation to cosmic acceleration for the apparent dimming of distant SNe of type Ia [60]. However, this dimming would apply to all distant sources, including quasars and the cosmic microwave background radiation, and would depend on energy. All things considered, this mechanism can only play a subdominant role [61].

High-energy  $\gamma$ -rays are typically produced in magnetized environments where cosmic rays are accelerated. The conversion into axion-like particles can then, in principle, imprint observable features on the spectrum for a range of coupling constants not excluded by other arguments [62].

## IV. COSMIC AXIONS

***IV.1 Cosmic axion populations:*** In the early universe, axions are produced by processes involving their couplings to quarks and gluons [63]. After the QCD confinement transition, the dominant thermalization process is  $\pi + \pi \leftrightarrow \pi + a$  [21]. The resulting cosmic axion population would contribute a hot dark-matter fraction in analogy to massive neutrinos. Cosmological precision data provide restrictive constraints on a possible hot dark-matter fraction that translate into  $m_A < 0.4\text{--}1.2 \text{ eV}$  at the 95% statistical CL [64]. The spread of the published limits reflects the use of different cosmological data. Including Lyman- $\alpha$  data leads to more restrictive limits that are, however, vulnerable to poorly controlled systematic uncertainties.

For  $m_A \gtrsim 20$  eV, axions decay into photons faster than a cosmic time scale, removing the axion population while injecting radiation. This excess radiation provides additional limits up to very large axion masses [65]. An anomalously small  $G_{A\gamma\gamma}$  provides no loophole because suppressing decays leads to thermal axions overdominating the mass density of the universe.

The main cosmological interest in axions derives from their possible role as cold dark matter (CDM). In addition to thermal processes, axions are abundantly produced by the “misalignment mechanism” [66]. After the spontaneous breakdown of the PQ symmetry at high energies, the axion field relaxes somewhere in the “bottom of the wine bottle” potential. Near the QCD epoch, instanton effects explicitly break the PQ symmetry, the very effect that causes the dynamical PQ symmetry restoration. This “tilting of the wine bottle bottom” causes the axion field to roll toward the  $CP$ -conserving minimum, thereby exciting coherent oscillations of the axion field that ultimately represent a “condensate” of CDM. The cosmic mass density in this homogeneous field mode is [67]

$$\Omega_A h^2 \approx 0.7 \left( \frac{f_A}{10^{12} \text{ GeV}} \right)^{7/6} \left( \frac{\bar{\Theta}_i}{\pi} \right)^2, \quad (17)$$

where  $h$  is the present-day Hubble expansion parameter in units of  $100 \text{ km s}^{-1} \text{ Mpc}^{-1}$ , and  $-\pi \leq \bar{\Theta}_i \leq \pi$  is the initial “misalignment angle” relative to the  $CP$ -conserving position. If the PQ symmetry breakdown takes place after inflation,  $\bar{\Theta}_i$  will take on different values in different patches of the universe. The average contribution is [67]

$$\Omega_A h^2 \approx 0.3 \left( \frac{f_A}{10^{12} \text{ GeV}} \right)^{7/6}. \quad (18)$$

Comparing with the measured CDM density of  $\Omega_{\text{CDM}} h^2 \approx 0.13$  implies that axions with  $m_A \approx 10 \mu\text{eV}$  provide the dark matter, whereas smaller masses are excluded (Figure 2).

This density sets only a crude scale of the expected  $m_A$ . Apart from the overall particle physics uncertainties, the cosmological sequence of events plays a crucial role. Assuming axions

make up CDM, significantly smaller masses are possible if inflation took place after the PQ transition and the initial value  $\bar{\Theta}_i$  was small. Conversely, if the PQ transition took place after inflation, there are additional sources for nonthermal axions, notably the formation and decay of cosmic strings and domain walls. However, these populations are comparable to the misalignment contribution [67]. Still, the mass of CDM axions could be significantly smaller or larger than  $10 \mu\text{eV}$  [67].

If the reheat temperature after inflation is too small to restore the PQ symmetry, the axion field is present during inflation, and subject to quantum mechanical fluctuations that lead to isocurvature fluctuations that are severely constrained by precision cosmological data [67,68]. One consequence is that the cosmic axion population cannot be arbitrarily small, even for a very small initial  $\bar{\Theta}_i$ .

In the opposite case without inflation after the PQ transition, the spatial axion density variation is large at the QCD transition. These density variations are not erased by free streaming. When matter begins to dominate the universe, gravitationally bound “axion mini clusters” form promptly [69]. A significant fraction of CDM axions can reside in these objects.

The hot and cold cosmic axion populations are not entirely independent. Most cold axions are produced shortly before the QCD phase transition. For  $f_A \lesssim 10^8 \text{ GeV}$ , axions reach thermal equilibrium after this epoch, thermalizing the axion field, thereby erasing the cold populations.

**IV.2 Telescope searches:** The two-photon decay rate of cosmic axions is extremely slow for axions with masses in the CDM regime, but could be detectable for eV-mass axions. The signature would be a quasi-monochromatic emission line from galaxies and galaxy clusters. This line, corrected for the host Doppler shift, would appear at half the axion mass, and its width would be similar to the virial width of objects in the host. The expected optical line intensity for DFSZ axions is similar to the continuum night emission. An early search in three rich Abell clusters [70], and a recent search in two rich Abell clusters [71], exclude the “Telescope” range in Figure 2 unless the axion–photon coupling is strongly suppressed. Of course,

axions in this mass range would also provide an excessive hot DM contribution.

Very low-mass axions in halos produce a weak quasi-monochromatic spectral line in the radio. Virial velocities in undisrupted dwarf galaxies are very low, and the axion emission line would therefore be extremely narrow. A search with the Haystack radio telescope on three nearby dwarf galaxies provided a limit  $G_{A\gamma\gamma} < 1.0 \times 10^{-9} \text{ GeV}^{-1}$  at 96% CL for  $298 < m_A < 363 \text{ } \mu\text{eV}$  [72]. However, this combination of  $m_A$  and  $G_{A\gamma\gamma}$  does not yet include plausible axion models.

**IV.3 Microwave cavity experiments:** The astrophysical and cosmological limits of Figure 2 suggest that axions, if they exist, provide a significant fraction or all of the cosmic CDM. In a broad range of the plausible  $m_A$  range for CDM axions, galactic halo axions may be detected by their resonant conversion into a quasi-monochromatic microwave signal in a high-Q electromagnetic cavity permeated by a strong static magnetic field [22,73]. The cavity frequency is tunable, and the signal is maximized when the frequency is the total axion energy, rest mass plus kinetic energy, of  $\nu = (m_A/2\pi)[1 + \mathcal{O}(10^{-6})]$ , the width above the rest mass representing the virial axion distribution in the galactic gravitational potential. The frequency spectrum width may also have finer structure from axions more recently fallen into the galactic potential and not yet completely virialized [74].

The feasibility of this technique was established in early experiments of relatively small sensitive volume,  $\mathcal{O}(1 \text{ liter})$  [75], with HFET-based amplifiers, setting limits in the range  $4.5 < m_A < 16.3 \text{ } \mu\text{eV}$ , but lacking by 2–3 orders of magnitude the sensitivity required to detect realistic axions. ADMX, a later experiment ( $B \sim 8 \text{ T}$ ,  $V \sim 200 \text{ liters}$ ) has achieved sensitivity to KSVZ axions, assuming they saturate the local dark matter halo and are well virialized, over the mass range  $1.9\text{--}3.3 \text{ } \mu\text{eV}$  [76]. Should halo axions have a component not yet virialized, ADMX is sensitive to DFSZ axions [77]. The corresponding 90% CL exclusion regions shown in Figure 4 are normalized to an assumed local CDM density of

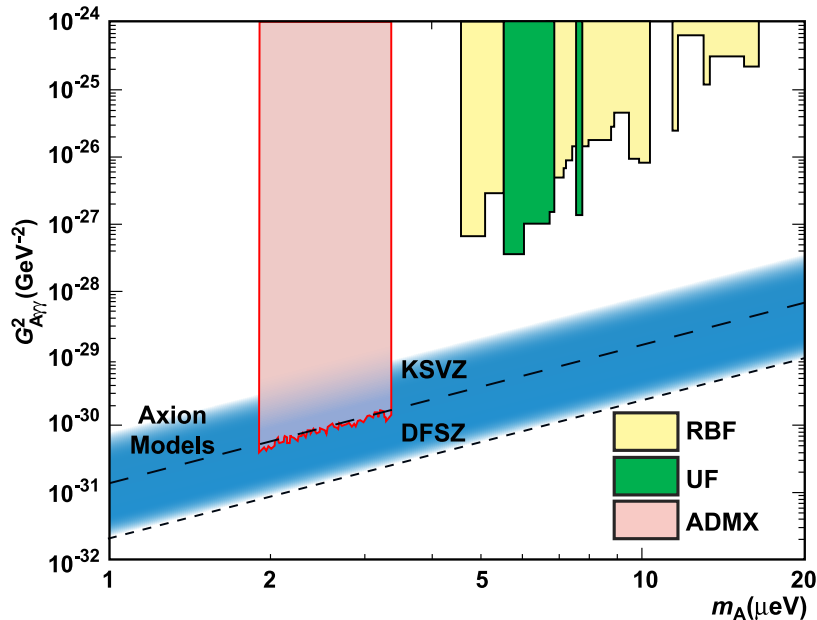


**Figure 4:** Exclusion region reported from the microwave cavity experiments RBF and UF [75] and ADMX [76]. A local dark-matter density of  $450 \text{ MeV cm}^{-3}$  is assumed.

$7.5 \times 10^{-25} \text{ g cm}^{-3}$  ( $450 \text{ MeV cm}^{-3}$ ) [78]. The ADMX experiment is currently undergoing commissioning of an upgrade that replaces the microwave HFET amplifiers by near quantum-limited low-noise dc SQUID amplifiers [79], allowing a significant improvement in the experiment sensitivity. A Rydberg atom single-photon detector [80] can in principle evade the standard quantum limit [81] for coherent detection, thus achieving very good sensitivity. Efforts are underway to incorporate Rydberg atom systems in RF cavity axion searches [82].

**Conclusions:** Experimental, astrophysical, and cosmological limits have been refined and indicate that axions, if they exist, are likely very light,  $m_A \lesssim 10 \text{ meV}$ , suggesting that axions are a non-negligible fraction of the cosmic CDM. The upgraded versions of the ADMX experiment will ultimately cover the range 1–100  $\mu\text{eV}$  with a sensitivity allowing one to detect axions, unless the local DM density is unexpectedly small or the axion–photon coupling anomalously weak. Other

experimental techniques remain of interest to search for general axion-like particles, although at present no method besides the DM search is known that could detect realistic axions obeying the astrophysical and cosmological limits, and fulfilling the QCD-implied relationship between mass and coupling strength.

## References

1. R.D. Peccei and H. Quinn, Phys. Rev. Lett. **38**, 1440 (1977), Phys. Rev. **D16**, 1791 (1977).
2. S. Weinberg, Phys. Rev. Lett. **40**, 223 (1978);  
F. Wilczek, Phys. Rev. Lett. **40**, 279 (1978).
3. F. Wilczek, Phys. Rev. Lett. **49**, 1549 (1982).
4. Y. Chikashige, R.N. Mohapatra, and R.D. Peccei, Phys. Lett. **98B**, 265 (1981);  
G.B. Gelmini and M. Roncadelli, Phys. Lett. **99B**, 411 (1981).
5. C.A. Baker *et al.*, Phys. Rev. Lett. **97**, 131801 (2006).
6. H. Georgi, D.B. Kaplan, and L. Randall, Phys. Lett. **B169**, 73 (1986).
7. H. Leutwyler, Phys. Lett. **B378**, 313 (1996).
8. W.M. Yao *et al.*, (Particle Data Group), J. Phys. G: Nucl. Part. Phys. **33**, 1 (2006).
9. T.W. Donnelly *et al.*, Phys. Rev. **D18**, 1607 (1978);  
S. Barshay *et al.*, Phys. Rev. Lett. **46**, 1361 (1981);  
A. Barroso and N.C. Mukhopadhyay, Phys. Lett. **B106**, 91 (1981);  
R.D. Peccei, in *Proceedings of Neutrino '81*, Honolulu, Hawaii, Vol. 1, p. 149 (1981);  
L.M. Krauss and F. Wilczek, Phys. Lett. **B173**, 189 (1986).
10. J. Schweppe *et al.*, Phys. Rev. Lett. **51**, 2261 (1983);  
T. Cowan *et al.*, Phys. Rev. Lett. **54**, 1761 (1985).
11. R.D. Peccei, T.T. Wu, and T. Yanagida, Phys. Lett. **B172**, 435 (1986).
12. W.A. Bardeen, R.D. Peccei, and T. Yanagida, Nucl. Phys. **B279**, 401 (1987).
13. J.E. Kim, Phys. Rev. Lett. **43**, 103 (1979);  
M.A. Shifman, A.I. Vainstein, and V.I. Zakharov, Nucl. Phys. **B166**, 493 (1980).
14. M. Dine, W. Fischler, and M. Srednicki, Phys. Lett. **B104**, 199 (1981);  
A.R. Zhitnitsky, Sov. J. Nucl. Phys. **31**, 260 (1980).

15. K.S. Choi, I.W. Kim, and J.E. Kim, JHEP **0703**, 116 (2007).
16. S.L. Cheng, C.Q. Geng, and W.T. Ni, Phys. Rev. **D52**, 3132 (1995).
17. G. Raffelt and D. Seckel, Phys. Rev. Lett. **60**, 1793 (1988);  
M. Carena and R.D. Peccei, Phys. Rev. **D40**, 652 (1989);  
K. Choi, K. Kang, and J.E. Kim, Phys. Rev. Lett. **62**, 849 (1989).
18. V.Y. Alexakhin *et al.*, (COMPASS Collaboration), Phys. Lett. **B647**, 8 (2007).
19. A. Airapetian *et al.*, (HERMES Collaboration), Phys. Rev. **D75**, 012007 (2007) and Erratum *ibid.*, **D76**, 039901 (2007).
20. J.R. Ellis and M. Karliner, in: *The spin structure of the nucleon: International school of nucleon structure (3–10 August 1995, Erice, Italy)*, ed. by B. Frois, V.W. Hughes, and N. De Groot (World Scientific, Singapore, 1997) [[hep-ph/9601280](#)].
21. S. Chang and K. Choi, Phys. Lett. **B316**, 51 (1993).
22. P. Sikivie, Phys. Rev. Lett. **51**, 1415 (1983) and Erratum *ibid.*, **52**, 695 (1984).
23. D.A. Dicus *et al.*, Phys. Rev. **D18**, 1829 (1978).
24. G. Raffelt and L. Stodolsky, Phys. Rev. **D37**, 1237 (1988).
25. K. van Bibber *et al.*, Phys. Rev. Lett. **59**, 759 (1987).
26. G. Ruoso *et al.*, Z. Phys. **C56**, 505 (1992);  
R. Cameron *et al.*, Phys. Rev. **D47**, 3707 (1993).
27. A. Afanasev *et al.*, [arXiv:hep-ph/0605250](#).
28. C. Robilliard *et al.*, Phys. Rev. Lett. **99**, 190403 (2007).
29. A.S. Chou *et al.* (GammeV Collab.), Phys. Rev. Lett. **100**, 080402 (2008).
30. P. Sikivie, D. Tanner, and K. van Bibber, Phys. Rev. Lett. **98**, 172002 (2007).
31. L. Maiani *et al.*, Phys. Lett. **B175**, 359 (1986).
32. Y. Semertzidis *et al.*, Phys. Rev. Lett. **64**, 2988 (1990).
33. E. Zavattini *et al.*, (PVLAS Collab.), Phys. Rev. Lett. **96**, 110406 (2006).
34. E. Zavattini *et al.*, (PVLAS Collab.), Phys. Rev. **D77**, 032006 (2008).
35. E. Fischbach and C. Talmadge, Nature **356**, 207 (1992).
36. J.E. Moody and F. Wilczek, Phys. Rev. D **30**, 130(1984).
37. A.N. Youdin *et al.*, Phys. Rev. Lett. **77**, 2170 (1996);  
Wei-Tou Ni *et al.*, Phys. Rev. Lett. **82**, 2439 (1999);

- D.F. Phillips *et al.*, Phys. Rev. **D63**, 111101 (R)(2001);  
 B.R. Heckel *et al.*, (Eöt-Wash Collaboration), Phys. Rev. Lett. **97**, 021603 (2006).
38. M.S. Turner, Phys. Reports **197**, 67 (1990);  
 G.G. Raffelt, Phys. Reports **198**, 1 (1990).
39. G.G. Raffelt, *Stars as Laboratories for Fundamental Physics*, (Univ. of Chicago Press, Chicago, 1996).
40. G.G. Raffelt, Lect. Notes Phys. **741**, 51 (2008) (Springer Verlag).
41. H. Schlattl, A. Weiss, and G. Raffelt, Astropart. Phys. **10**, 353 (1999).
42. J.N. Bahcall, A.M. Serenelli, and S. Basu, Astrophys. J. **21**, L85 (2005).
43. Q.R. Ahmad *et al.*, (SNO Collaboration), Phys. Rev. Lett. **89**, 011301 (2002);  
 B. Aharmim *et al.*, (SNO Collaboration), Phys. Rev. **C72**, 055502 (2005).
44. A. Buzzoni *et al.*, Astron. Astrophys. **128**, 94 (1983).
45. G. Raffelt and A. Weiss, Phys. Rev. **D51**, 1495 (1995);  
 M. Catelan, J.A. de Freitas Pacheco, and J.E. Horvath, Astrophys. J. **461**, 231 (1996).
46. G.G. Raffelt, Phys. Lett. **B166**, 402 (1986);  
 S.I. Blinnikov and N.V. Dunina-Barkovskaya, Mon. Not. R. Astron. Soc. **266**, 289 (1994).
47. A.H. Córscico *et al.*, New Astron. **6**, 197 (2001);  
 J. Isern and E. García-Berro, Nucl. Phys. B Proc. Suppl. **114**, 107 (2003).
48. J. Engel, D. Seckel, and A.C. Hayes, Phys. Rev. Lett. **65**, 960 (1990).
49. T. Moroi and H. Murayama, Phys. Lett. **B440**, 69 (1998).
50. K. van Bibber *et al.*, Phys. Rev. **D39**, 2089 (1989).
51. D. Lazarus *et al.*, Phys. Rev. Lett. **69**, 2333 (1992).
52. S. Moriyama *et al.*, Phys. Lett. **B434**, 147 (1998);  
 Y. Inoue *et al.*, Phys. Lett. **B536**, 18 (2002).
53. K. Zioutas *et al.*, (CAST Collaboration), Phys. Rev. Lett. **94**, 121301 (2005);  
 S. Andriamonje *et al.*, (CAST Collaboration), JCAP **0704**, 010 (2007).
54. K. Zioutas *et al.*, (CAST Collaboration), “Status Report of the CAST experiment and request to run beyond 2007,” CERN-SPSC-2007-013 (5 April 2007), see <http://doc.cern.ch/archive/electronic/cern/preprints/spsc/public/spsc-2007-013.pdf>.

55. F.T. Avignone III *et al.*, Phys. Rev. Lett. **81**, 5068 (1998).
56. A. Morales *et al.*, (COSME Collaboration), Astropart. Phys. **16**, 325 (2002).
57. R. Bernabei *et al.*, Phys. Lett. **B515**, 6 (2001).
58. H. Davoudiasl and P. Huber, Phys. Rev. Lett. **97**, 141302 (2006).
59. J.W. Brockway, E.D. Carlson, and G.G. Raffelt, Phys. Lett. **B383**, 439 (1996);  
J.A. Grifols, E. Massó, and R. Toldrà, Phys. Rev. Lett. **77**, 2372 (1996).
60. C. Csaki, N. Kaloper, and J. Terning, Phys. Rev. Lett. **88**, 161302 (2002).
61. A. Mirizzi, G.G. Raffelt, and P.D. Serpico, Lect. Notes Phys. **741**, 115 (2008).
62. D. Hooper and P.D. Serpico, Phys. Rev. Lett. **99**, 231102 (2007);  
K.A. Hochmuth and G. Sigl, Phys. Rev. **D76**, 123011 (2007).
63. M.S. Turner, Phys. Rev. Lett. **59**, 2489 (1987) and Erratum *ibid.*, **60**, 1101 (1988);  
E. Massó, F. Rota, and G. Zsembinszki, Phys. Rev. **D66**, 023004 (2002).
64. S. Hannestad, A. Mirizzi, and G. Raffelt, JCAP **0507**, 002 (2005);  
A. Melchiorri, O. Mena, and A. Slosar, Phys. Rev. **D76**, 041303 (2007);  
S. Hannestad *et al.*, JCAP **0708**, 015 (2007).
65. E. Massó and R. Toldrà, Phys. Rev. **D55**, 7967 (1997).
66. J. Preskill, M.B. Wise, and F. Wilczek, Phys. Lett. **B120**, 127 (1983);  
L.F. Abbott and P. Sikivie, Phys. Lett. **B120**, 133 (1983);  
M. Dine and W. Fischler, Phys. Lett. **B120**, 137 (1983).
67. P. Sikivie, Lect. Notes Phys. **741**, 19 (2008).
68. M. Beltrán, J. García-Bellido, and J. Lesgourgues, Phys. Rev. **D75**, 103507 (2007).
69. E.W. Kolb and I.I. Tkachev, Phys. Rev. Lett. **71**, 3051 (1993);  
E.W. Kolb and I.I. Tkachev, Astrophys. J. **460**, L25 (1996).
70. M. Bershadsky *et al.*, Phys. Rev. Lett. **66**, 1398 (1991);  
M. Ressel, Phys. Rev. **D44**, 3001 (1991).
71. D. Grin *et al.*, Phys. Rev. **D5**, 105018 (2007).
72. B.D. Blout *et al.*, Astrophys. J. **546**, 825 (2001).

73. P. Sikivie, Phys. Rev. **D32**, 2988 (1985);  
L. Krauss *et al.*, Phys. Rev. Lett. **55**, 1797 (1985);  
R. Bradley *et al.*, Rev. Mod. Phys. **75**, 777 (2003).
74. P. Sikivie and J. Ipser, Phys. Lett. **B291**, 288 (1992);  
P. Sikivie *et al.*, Phys. Rev. Lett. **75**, 2911 (1995).
75. S. DePanfilis *et al.*, Phys. Rev. Lett. **59**, 839 (1987);  
W. Wuensch *et al.*, Phys. Rev. **D40**, 3153 (1989);  
C. Hagmann *et al.*, Phys. Rev. **D42**, 1297 (1990).
76. S. Asztalos *et al.*, Phys. Rev. **D69**, 011101 (2004).
77. L. Duffy *et al.*, Phys. Rev. Lett. **95**, 091304 (2005).
78. E. Gates *et al.*, Astrophys. J. **449**, 123 (1995).
79. M. Mück, J.B. Kycia, and J. Clarke, Appl. Phys. Lett. **78**,  
967 (2001).
80. I. Ogawa, S. Matsuki, and K. Yamamoto, Phys. Rev. **D53**,  
1740 (1996).
81. V. Braginsky and F. Khalili in: *Quantum Measurement*,  
ed. by K. Thorne (Cambridge University Press, Cam-  
bridge) 1992.
82. S. Matsuki *et al.*, Nucl. Phys. B (Proc. Suppl.) **51**, 213  
(1996);  
Y. Kishimoto *et al.*, Phys. Lett. **A303**, 279 (2002);  
M. Tada *et al.*, Phys. Lett. **A303**, 285 (2002).